Electronic Supplementary Material (ESI) for Nanoscale.

Supporting information for

A squaraine-linked zwitterionic COF modified LLZTO nanoparticles for high performance polymer composite electrolyte in Li-S battery

Shuo Wang, Mengke Li, Gaojie Yan, Zhipeng Yang, Yuchao Guo, Xi Sun, Yue Wang, Yi Feng*, Huili Ding*, and Xiaojie Zhang*

Hebei Key Laboratory of Functional Polymers, Department of Polymer Materials and Engineering, Hebei University of Technology, Tianjin 300400, P. R. China

Corresponding author:

*Email: luckyii0512@hebut.edu.cn (Y. Feng)

*Email: aleeding@hebut.edu.cn (H. Ding)

*Email: zhangxj@hebut.edu.cn (X. Zhang)

Decision on the mass ratio of raw materials for preparing LLZTO@HUT4 nanoparticles

Ionic conductivity and transference number were measured for obtained PCEs with LLZTO@HUT4 nanoparticles synthesized via different mass ratios of raw materials. The total mass of squaric acid and melamine monomers was denoted as M_{SM}, and the mass of LLZTO powders was denoted as M_{LLZTO}. Nyquist plots and Chronoamperometric curves of PCEs with different mass ratios (M_{LLZTO}: M_{SM} = 3:1, 2:1, 1:1, 1:2) were shown in **Fig. S4** and **S5**, it demonstrated that the LLZTO@HUT4/PEO electrolyte with M_{LLZTO}: M_{SM} = 2:1 exhibited higher ionic conductivity (0.52 mS cm^{-1}) than other ratios. Moreover, the transference number of as-prepared electrolytes were calculated as presented in **Table S2**. when M_{LLZTO}: M_{SM} = 2:1, the electrolyte exhibited the highest transference number (0.51) at 60 °C compared with other counterparts. Therefore, the mass ratio of M_{LLZTO}: M_{SM} = 2:1 was applied in further experiments.

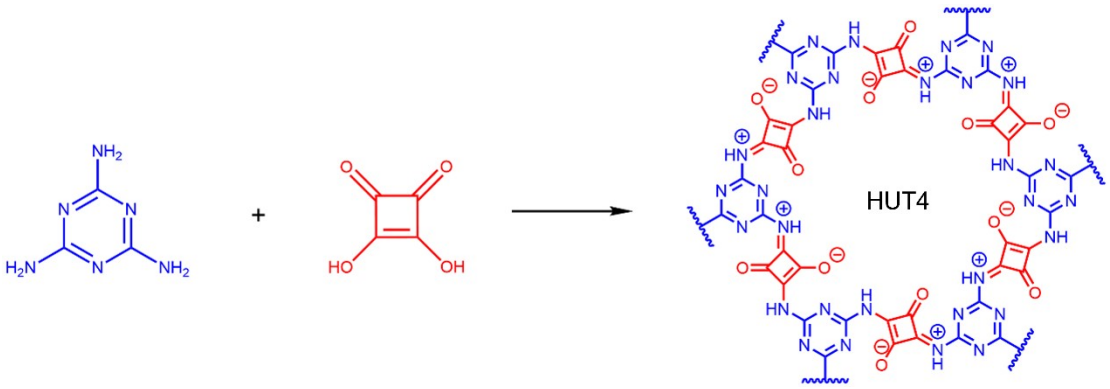

Fig. S1. The synthetic route of HUT4.

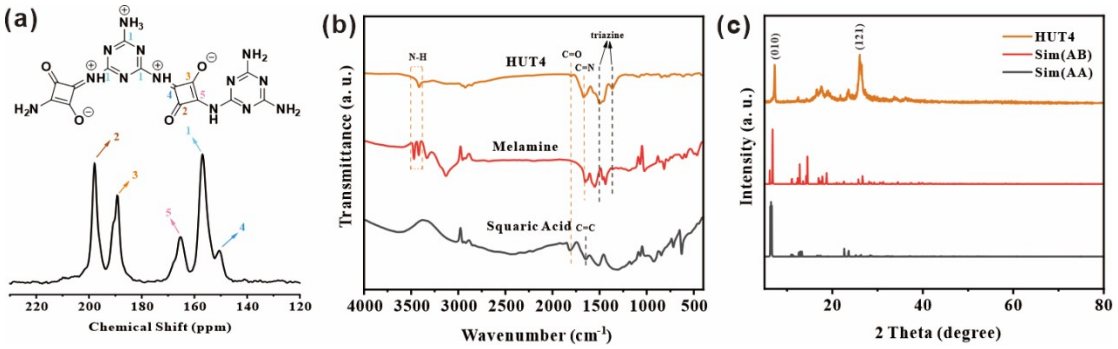

Fig. S2. (a) Solid-state ^{13}C NMR of HUT4; (b) FTIR spectra of squaric acid, melamine and HUT4; (c) Experimental and simulated XRD patterns of HUT4.

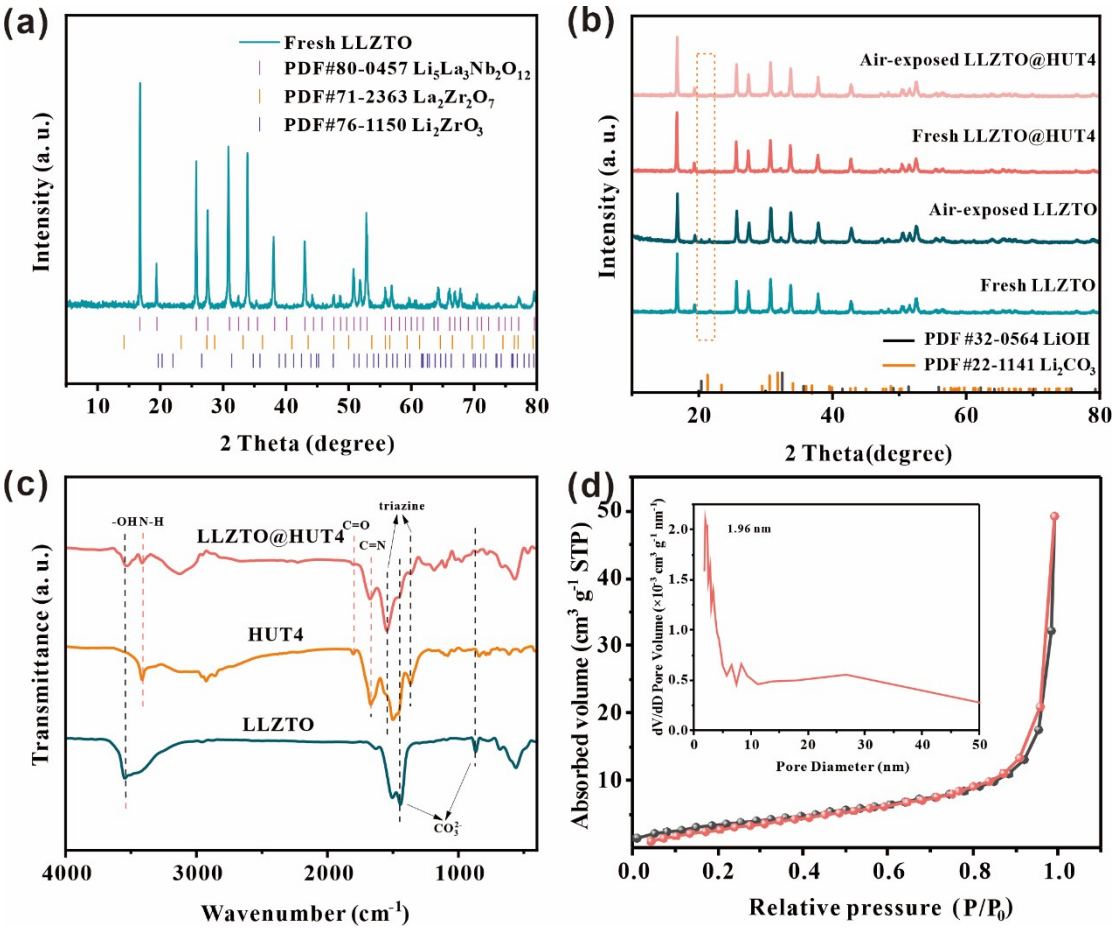

Fig. S3. (a) XRD patterns of fresh LLZTO and PDF of Cubic garnet (98.3%), $La_2Zr_2O_7$ (1.7%), Li_2ZrO_3 (0%), the relative content was obtained by fitting with Jade; (b) XRD patterns of fresh LLZTO, 2 days air-exposed LLZTO, fresh LLZTO@HUT4 and 30 days air-exposed LLZTO@HUT4; (c) FTIR spectra of LLZTO, HUT4 and LLZTO@HUT4; (d) Nitrogen isotherm adsorption and desorption curve of LLZTO@HUT4 (inset: Pore size distribution profiles of LLZTO@HUT4).

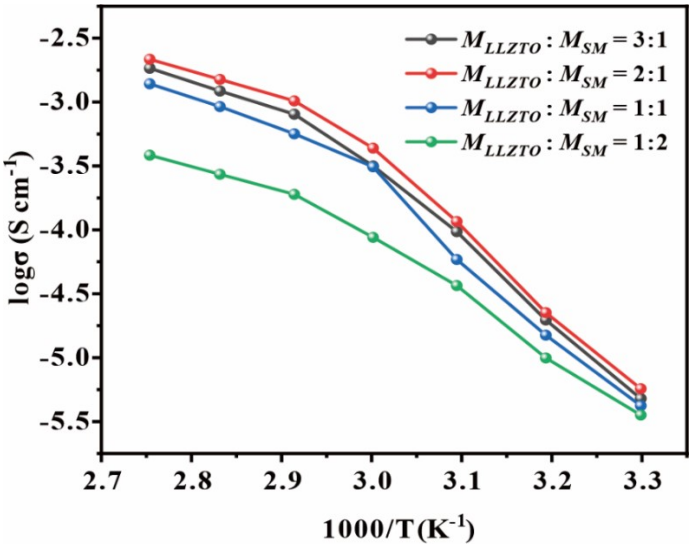

Fig. S4. Arrhenius plots of ionic conductivity for PCEs prepared with LLZTO@HUT4 nanoparticles in various M_{LLZTO} to M_{SM} ratios.

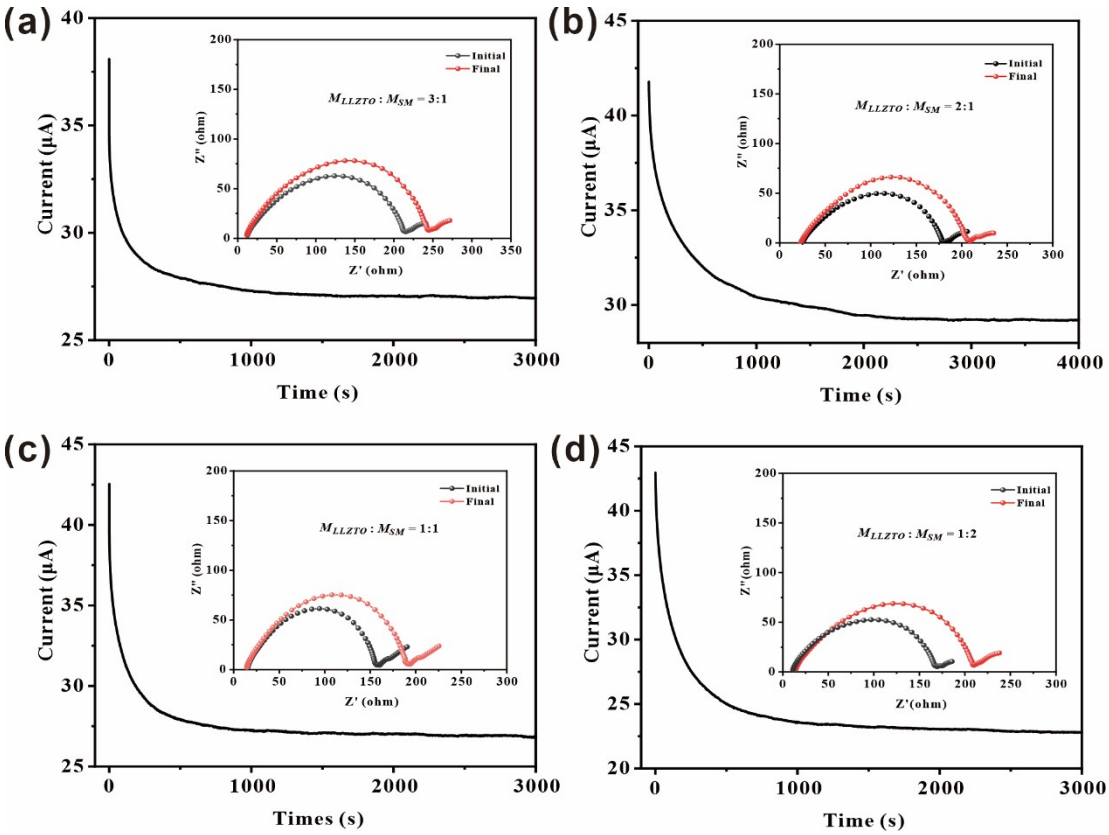

Fig. S5. Chronoamperometric curves and EIS Nyquist plots of PCEs prepared in different M_{LLZTO} to M_{SM} mass ratios at 60 °C: (a) M_{LLZTO}: M_{SM} = 3:1; (b) M_{LLZTO}: M_{SM} = 2:1; (c) M_{LLZTO}: M_{SM} = 1:1; (d) M_{LLZTO}: M_{SM} = 1:2.

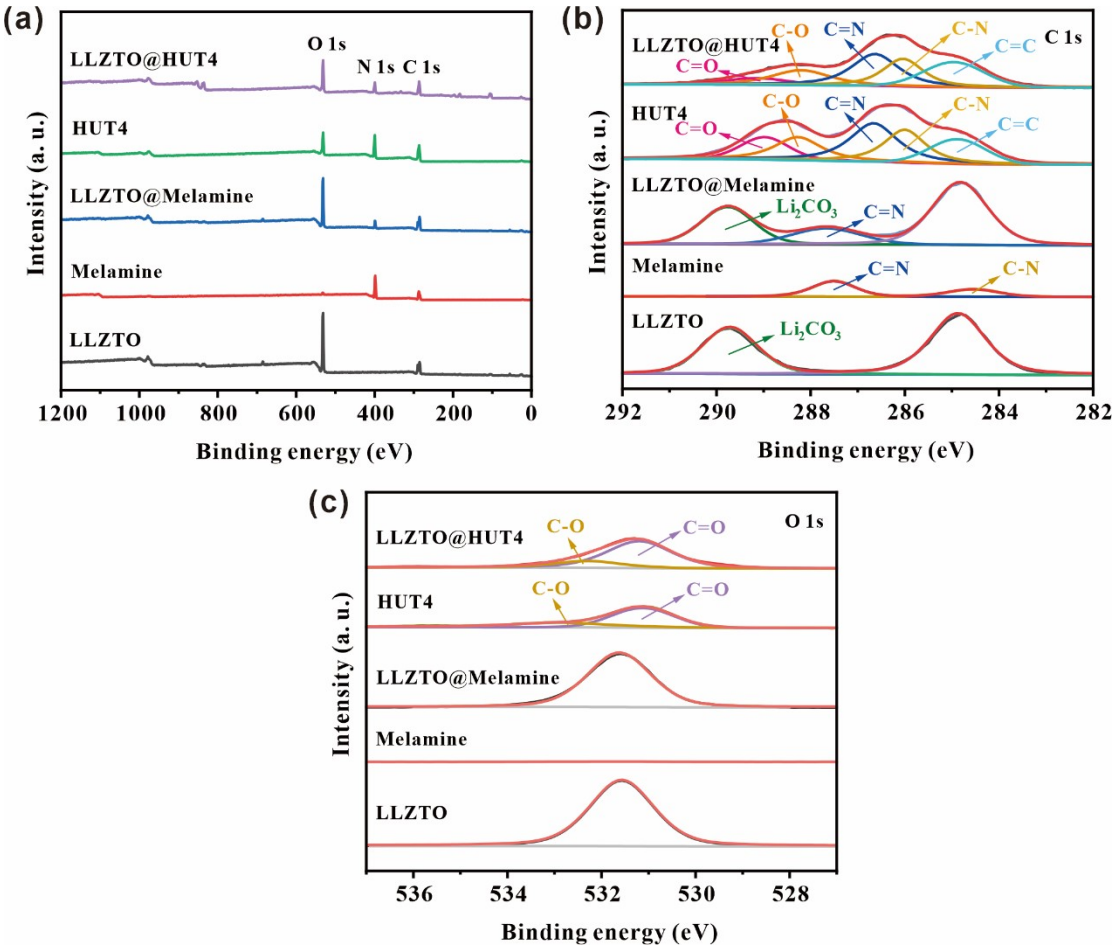

Fig. S6. (a) XPS survey, (b) C 1s and (c) O 1s spectra of air-exposed LLZTO, Melamine, LLZTO@Melamine, HUT4 and LLZTO@HUT4 nanoparticles.

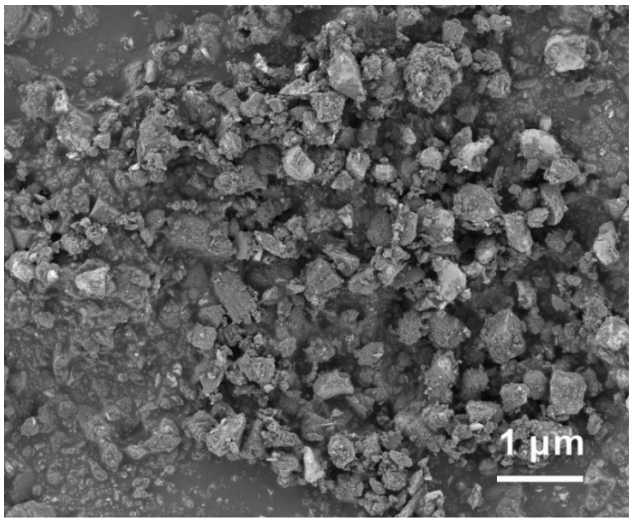

Fig. S7. SEM images of LLZTO@HUT4 nanoparticles.

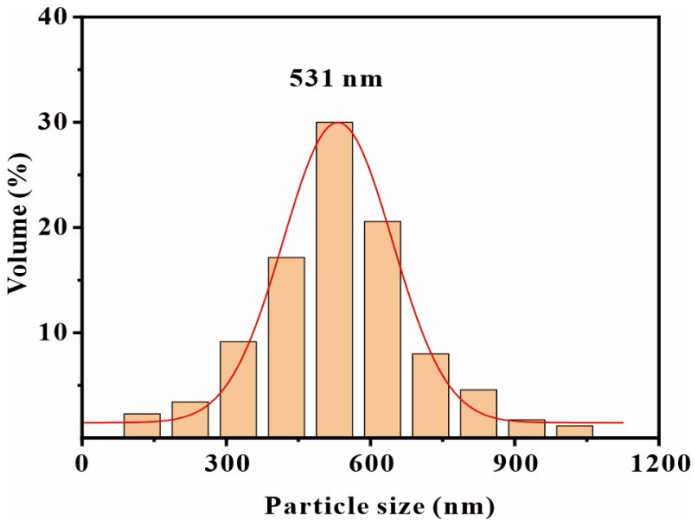

Fig. S8. Particles size distribution of the LLZTO powders.

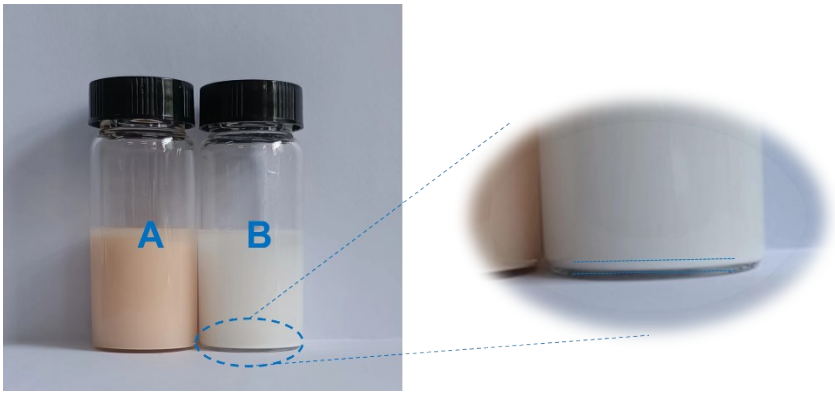

Fig. S9. Sedimentation experiment in PEO solvent. A is LLZTO@HUT4 and B is air-exposed LLZTO.

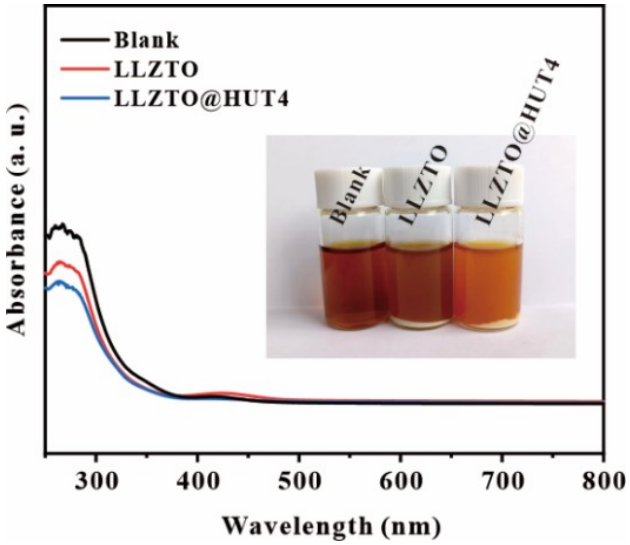

Fig. S10. UV-visible absorption spectra of blank, LLZTO, and LLZTO@HUT4 powder soaked in Li_2S_6 solution.

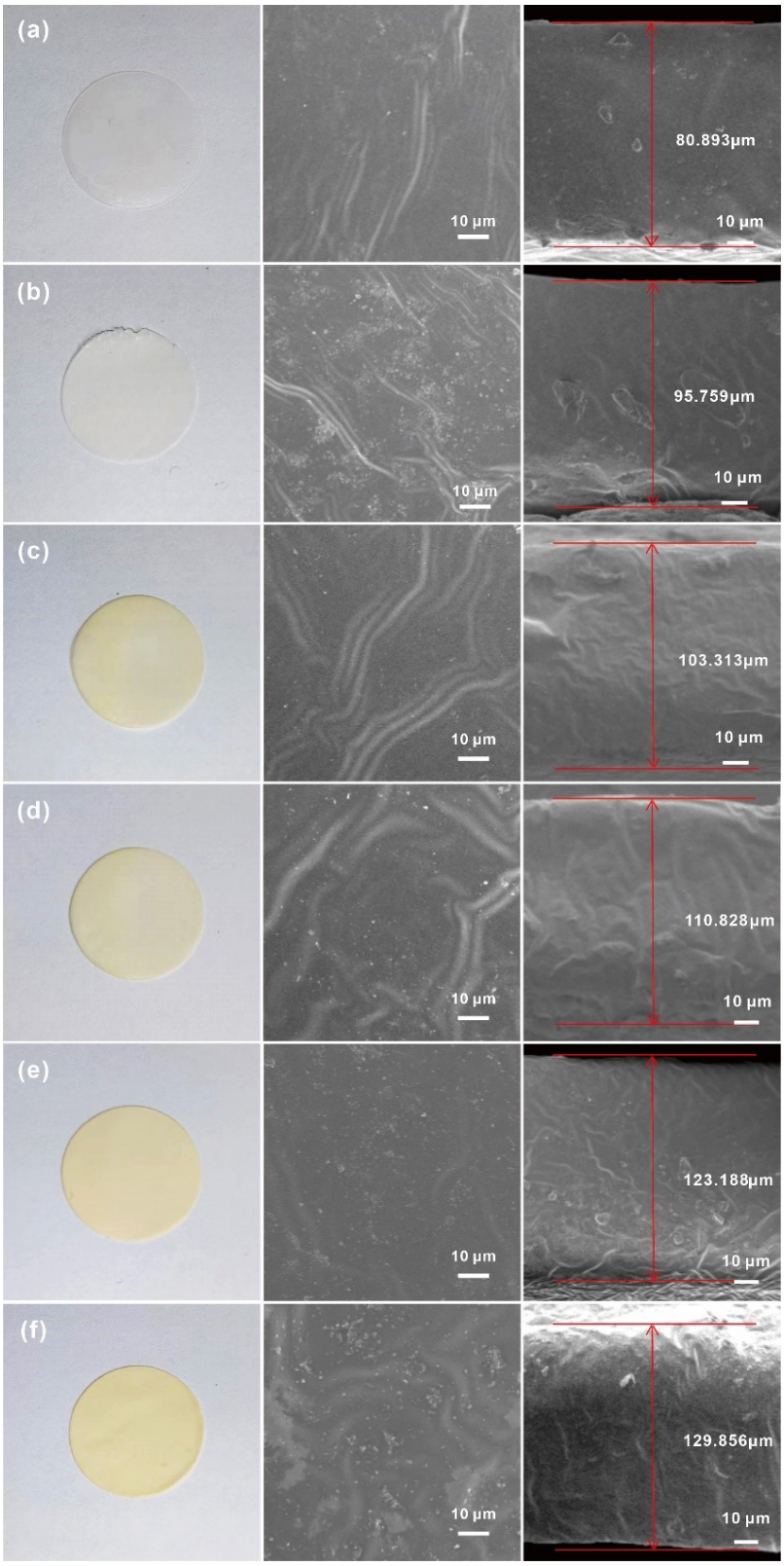

Fig. S11. Digital photographs and SEM images on the surface and cross section of synthesized PCEs: (a) PEO; (b) LLZTO-15%/PEO; (c) LLZTO@HUT4-5%/PEO; (d) LLZTO@HUT4-10%/PEO; (e) LLZTO@HUT4-15%/PEO; (f) LLZTO@HUT4-20%/PEO, respectively.

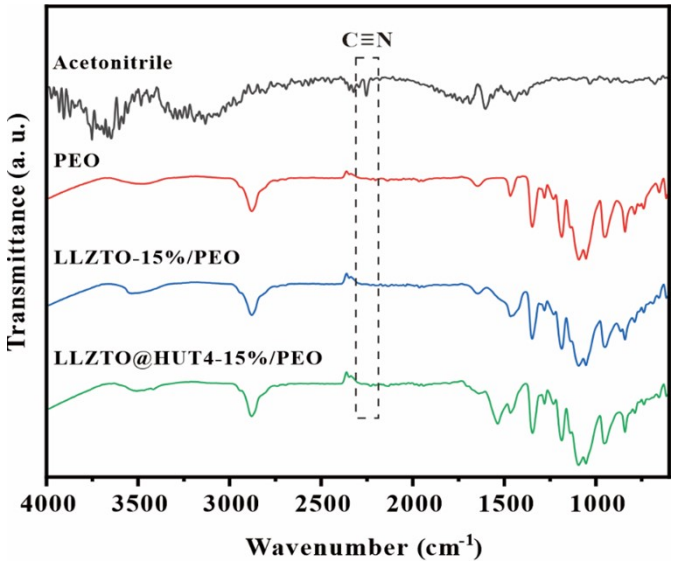

Fig. S12. ATR-FTIR spectra of acetonitrile, PEO, LLZTO-15%/PEO and LLZTO@HUT4-15%/PEO.

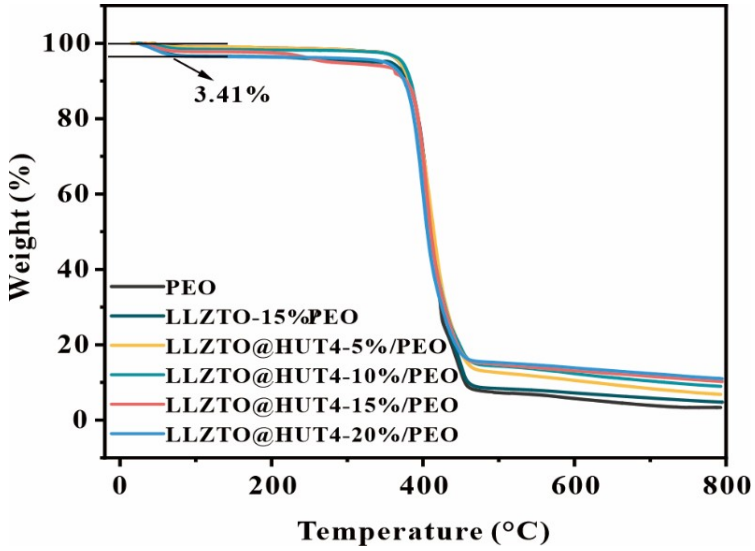

Fig. S13. TGA curves of PEO, LLZTO-15%/PEO and LLZTO@HUT4/PEO PCEs.

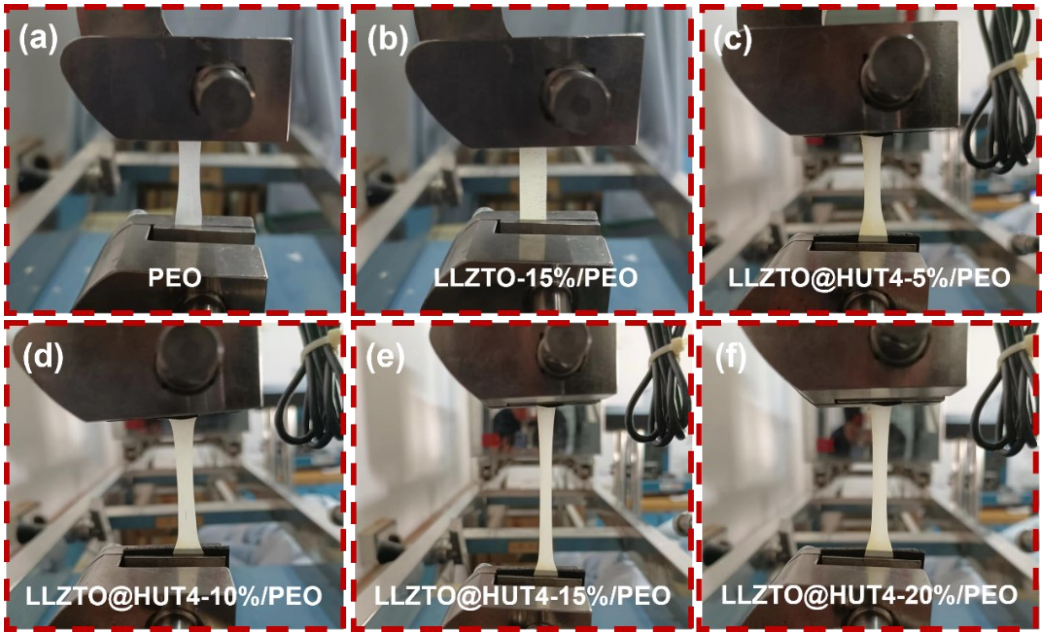

Fig. S14. Optical photos of tensile test of (a) PEO; (b) LLZTO-15%/PEO; (c) LLZTO@HUT4-5%/PEO; (d) LLZTO@HUT4-10%/PEO; (e) LLZTO@HUT4-15%/PEO; (f) LLZTO@HUT4-20%/PEO electrolytes.

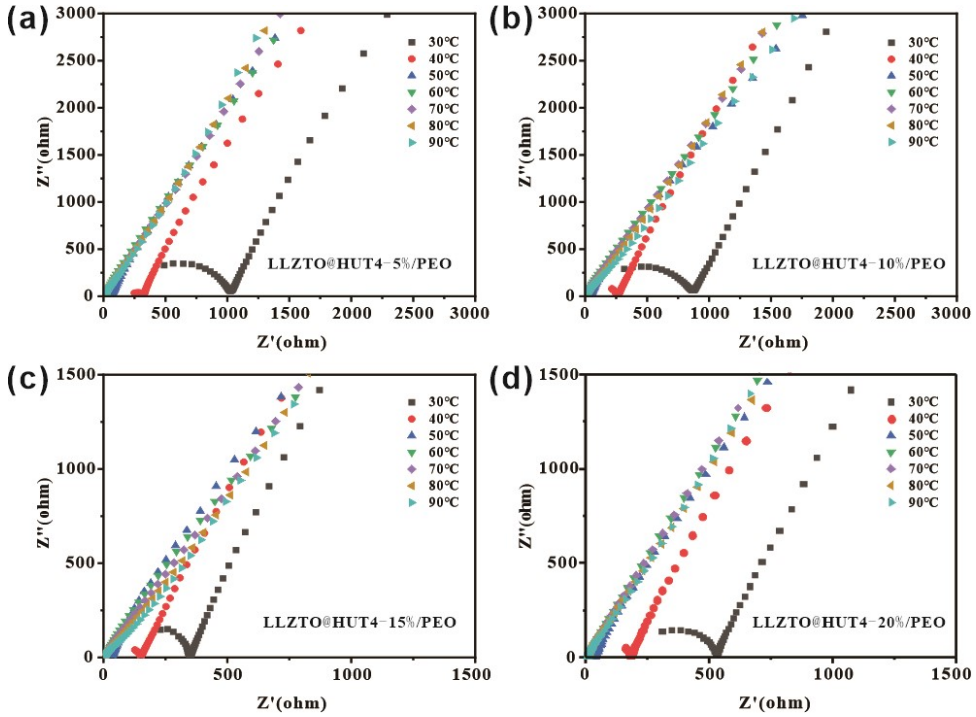

Fig. S15. Nyquist plots of LLZTO@HUT4/PEO evaluated in various temperatures (30 °C to 90 °C) with various LLZTO@HUT4 mass ratios: (a) LLZTO@HUT4-5%/PEO; (b) LLZTO@HUT4-10%/PEO; (c) LLZTO@HUT4-15%/PEO; (d) LLZTO@HUT4-20%/PEO.

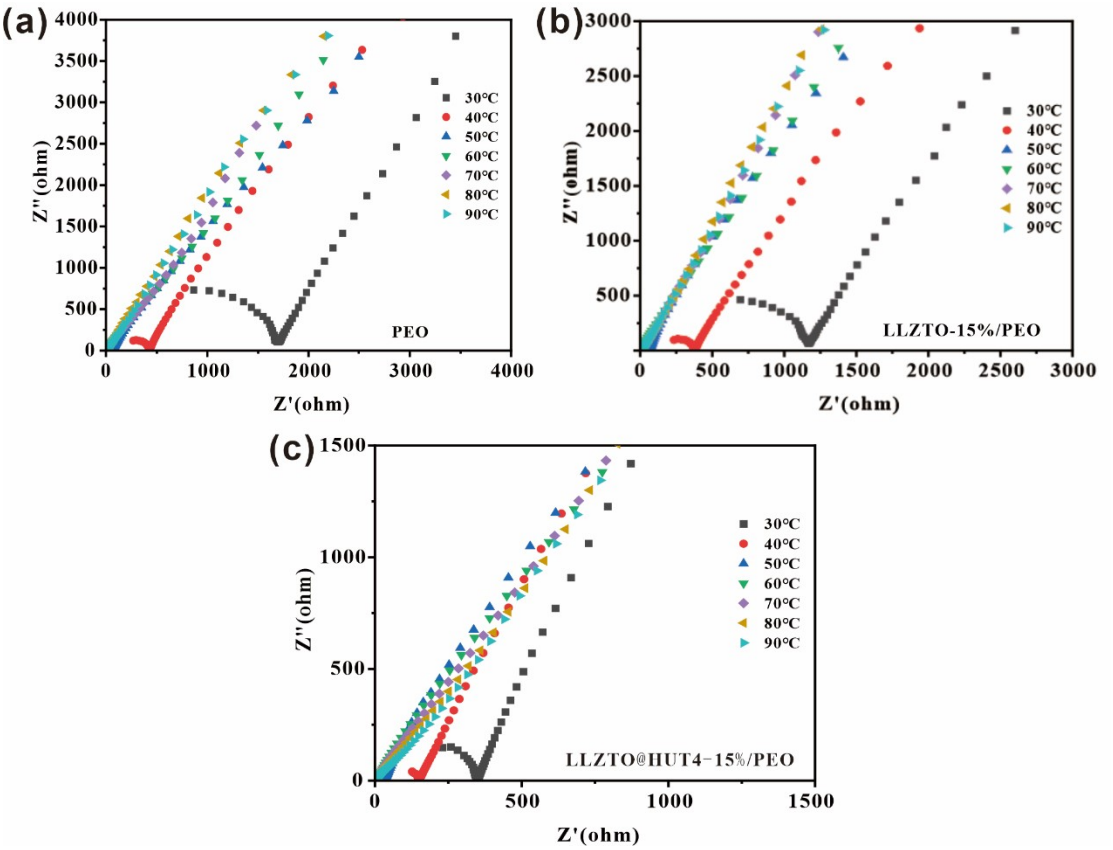

Fig. S16. EIS Nyquist plots of as synthesized PCEs evaluated in various temperatures (30 °C to 90 °C): (a) PEO; (b) LLZTO-15%/PEO; (c) LLZTO@HUT4-15%/PEO.

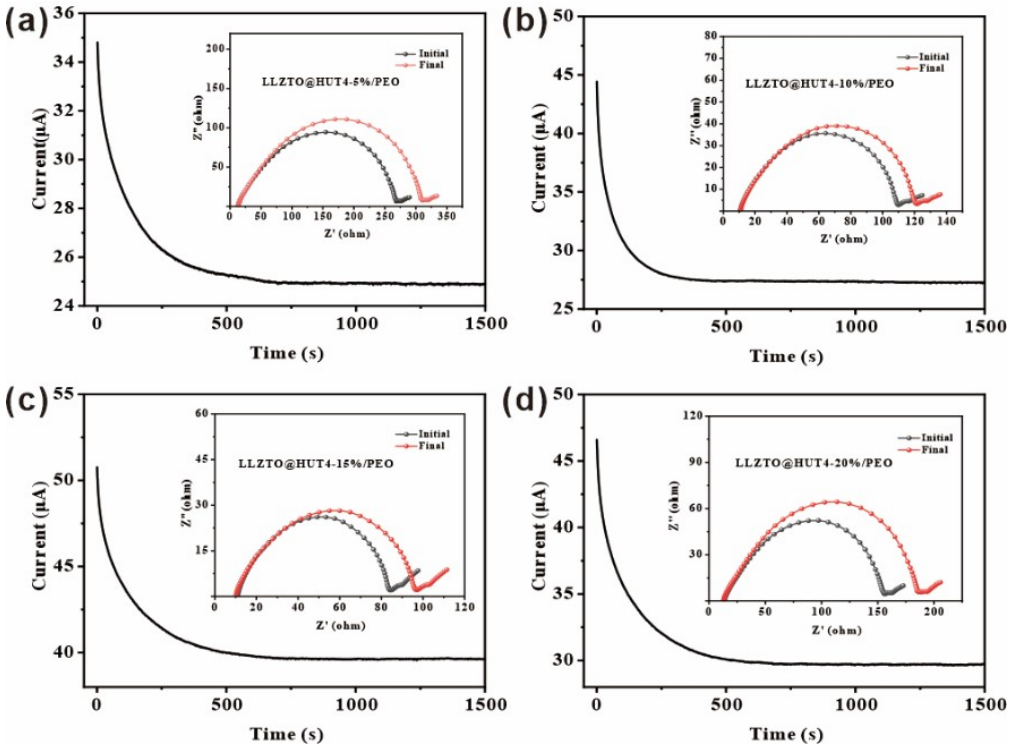

Fig. S17. Chronoamperometric curves and EIS Nyquist plots of (a) LLZTO@HUT4-5%/PEO; (b) LLZTO@HUT4-10%/PEO; (c) LLZTO@HUT4-15%/PEO; (d) LLZTO@HUT4-20%/PEO electrolytes at 60 °C.

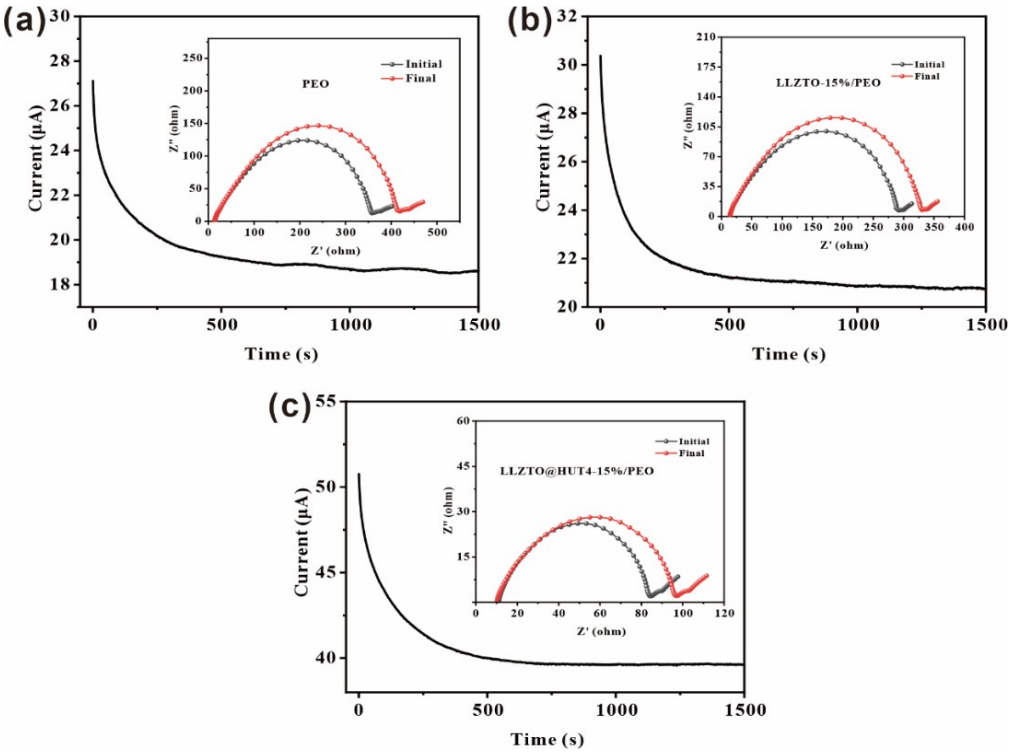

Fig. S18. Chronoamperometric curves and Nyquist plots of as synthesized PCEs at 60 °C: (a) PEO; (b) LLZTO-15%/PEO; (c) LLZTO@HUT4-15%/PEO.

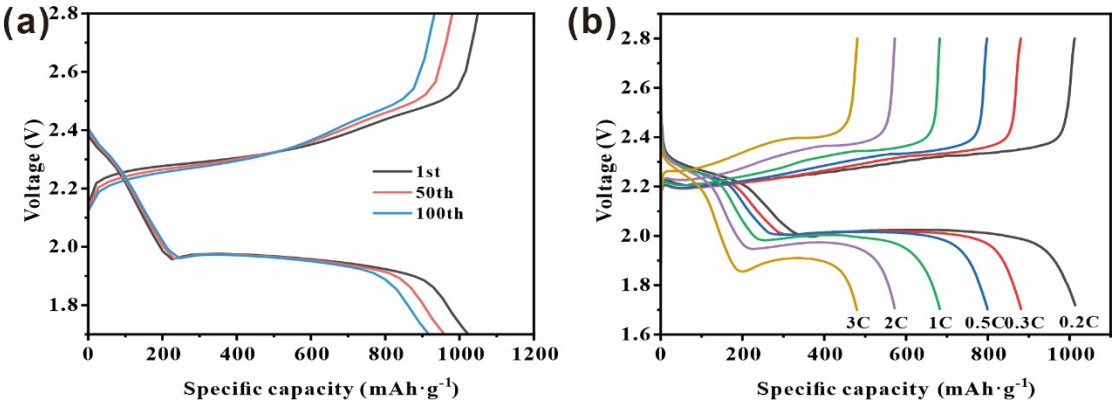

Fig. S19. (a) Discharge-charge profiles at 0.2 C for S@CNT|LLZTO@HUT4-15%/PEO|Li; (b) Discharge-charge curves of S@CNT|LLZTO@HUT4-15%/PEO|Li at 60 °C in different rates.

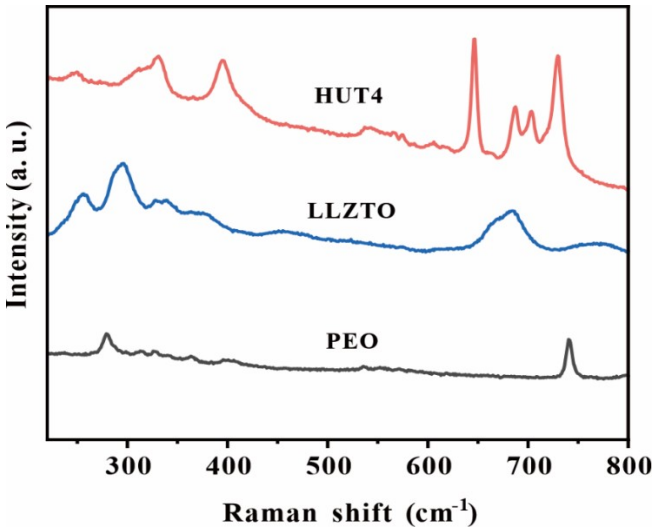

Fig. S20. Raman spectra of HUT4, LLZTO and PEO membrane.

Table S1. ICP-OES analysis results of LLZTO containing the weight and atomic ratios of metal element: Li, La, Zr and Ta

Metal elements	Weight ratio (%)	Atomic ratio (%)
Li	6.35	56.07
La	58.74	25.92
Zr	18.63	12.50
Ta	16.28	5.51

Table S2. Li^+ ions transference number of PCEs prepared with LLZTO@HUT4 nanoparticles in various mass ratios of M_{LLZTO} to M_{SM} at 60 °C.

	I_0/ μA	I_S/ μA	R_0/ Ω	R_S/ Ω	ΔV/ mV	t_{Li^+}
M_{LLZTO}: M_{SM} = 3:1	38.09	26.86	202.44	232.71	10	0.43
M_{LLZTO}: M_{SM} = 2:1	41.78	28.90	157.60	185.56	10	0.51
M_{LLZTO}: M_{SM} = 1:1	42.54	27.11	155.38	179.09	10	0.42
M_{LLZTO}: M_{SM} = 1:2	42.96	22.80	157.81	195.03	10	0.31

Table S3. DSC data of as synthesized PCEs

	T_m/ °C	ΔH_m/ J g^{-1}	χ_c/ %
PEO	57.05	65.80	44.67
LLZTO-15%/PEO	55.68	53.47	38.89
LLZTO@HUT4-5%/PEO	55.22	52.26	35.39
LLZTO@HUT4-10%/PEO	54.47	40.86	29.65
LLZTO@HUT4-15%/PEO	54.02	32.18	24.17
LLZTO@HUT4-20%/PEO	53.09	30.06	23.34

Table S4. Data of mechanical properties of PCEs

	Tensile strength/ MPa	**Percentage of breaking elongation/ %**
PEO	1.37	1753.44
LLZTO -15%/PEO	1.32	1095.01
LLZTO@HUT4-5%/PEO	1.34	1543.00
LLZTO@HUT4-10%/PEO	1.70	2149.55
LLZTO@HUT4-15%/PEO	2.40	2152.99
LLZTO@HUT4-20%/PEO	2.25	2084.30

Table S5. Ionic conductivity of PCEs with different ratios of LLZTO@HUT4 from 30 to 90 ℃ (Each ratio of the samples were tested 3 times and the average value was calculated, Unit: mS cm^{-1}).

	30 °C	**40 °C**	**50 °C**	**60 °C**	**70 °C**	**80 °C**	**90 °C**
LLZTO@HUT4-5%/PEO	0.0058	0.0059	0.016	0.28	0.68	1.20	1.79
	0.0049	0.0072	0.020	0.31	0.71	1.15	1.72
	0.0046	0.0064	0.018	0.28	0.62	1.07	1.86
	average	average	average	average	average	average	average
	0.0051	0.016	0.086	0.29	0.67	1.14	1.79
LLZTO@HUT4-10%/PEO	0.0073	0.022	0.13	0.55	0.93	1.59	2.11
	0.0064	0.019	0.16	0.49	0.98	1.52	2.01
	0.0058	0.025	0.13	0.55	0.97	1.48	2.15
	average	average	average	average	average	average	average
	0.0065	0.022	0.14	0.53	0.96	1.53	2.09
LLZTO@HUT4-15%/PEO	0.018	0.049	0.19	0.75	1.42	2.03	3.06
	0.015	0.038	0.17	0.72	1.32	1.94	3.02
	0.021	0.039	0.21	0.72	1.37	2.00	3.10
	average	average	average	average	average	average	average
	0.018	0.042	0.19	0.73	1.37	1.99	3.06
LLZTO@HUT4-20%/PEO	0.010	0.039	0.15	0.40	0.80	1.14	1.71
	0.016	0.040	0.17	0.46	0.69	1.20	1.59
	0.013	0.032	0.19	0.43	0.76	1.11	1.68
	average	average	average	average	average	average	average
	0.013	0.037	0.17	0.43	0.75	1.15	1.66

Table S6. Ionic conductivity of as-synthesized PCEs from 30 °C to 90 °C (Each sample was tested 3 times and the average value was calculated, Unit: mS cm^{-1}).

	30 °C	**40 °C**	**50 °C**	**60 °C**	**70 °C**	**80 °C**	**90 °C**
LLZTO	0.016	0.049	0.075	0.11	0.20	0.31	0.49
	0.017	0.045	0.081	0.14	0.23	0.30	0.52
	0.024	0.044	0.078	0.17	0.20	0.35	0.49
	average	average	average	average	average	average	average
	0.019	0.046	0.078	0.14	0.21	0.32	0.50
PEO	0.0020	0.0097	0.053	0.34	0.57	0.63	0.98
	0.0024	0.010	0.062	0.35	0.61	0.72	1.11
	0.0028	0.0091	0.065	0.27	0.53	0.69	0.94
	average	average	average	average	average	average	average
	0.0024	0.0096	0.060	0.32	0.57	0.68	1.01
LLZTO-10%/PEO	0.0045	0.012	0.082	0.39	0.67	0.99	1.42
	0.0040	0.013	0.082	0.35	0.66	0.97	1.50
	0.0038	0.014	0.076	0.40	0.62	1.10	1.55
	average	average	average	average	average	average	average
	0.0041	0.013	0.080	0.38	0.65	1.02	1.49
LLZTO@HUT4-15%/PEO	0.018	0.049	0.19	0.75	1.42	2.03	3.06
	0.015	0.038	0.17	0.72	1.32	1.94	3.02
	0.021	0.039	0.21	0.72	1.37	2.00	3.10
	average	average	average	average	average	average	average
	0.018	0.042	0.19	0.73	1.37	1.99	3.06

Table S7. The electrochemical data is cited in the reported literature of the PEO based electrolytes

Ref.	Electrolyte composition	t_{Li^+}	Ionic conductivity/ S cm^{-1}
This study	LLZTO@HUT4-15%/PEO	0.74	7.33×10^{-4} (60 °C)
1	PEO/LiTFSI	0.21	3.4×10^{-6} (25 °C)
2	PEO/LiTFSI/HUT4	0.62	5.3×10^{-4} (90 °C)
3	PEO-10%iCP@TFSI	0.284	1.2×10^{-3} (80 °C)
4	LiTFSI/PEO-IL@ZrO_2	/	4.95×10^{-4} (50 °C)
5	PEO/LiTFSI/Al_2O_3	0.43	5.4×10^{-4} (60 °C)
6	PVDF-HFP/$LiAlO_2$@g-Al_2O_3	0.92	8.5×10^{-4} (25 °C)
7	PEO/$LiClO_4$/TiO_2	/	5.308×10^{-5} (20 °C)
8	PEO/LiTFSI-15%LLZO	/	1.1×10^{-4} (40 °C)
9	PEO/EO@LLZTO	0.72	1.91×10^{-4} (60 °C)
10	PEO/LLZTO@CD-TFSI	0.48	8.7×10^{-4} (60 °C)
11	PEO/PVDF/LLZTO	0.3	9.3×10^{-4} (50 °C)
12	PEO/LLZTO@SA	/	8.3×10^{-4} (70 °C)
13	PEO/PPO@LLZTO	0.33	2.43×10^{-5} (60 °C)
14	PEO(10)/LLZTO(85)/PEG(5)	/	5.24×10^{-4} (80 °C)
15	PEO/LiTFSI/LLZTO(50vol)	< 0.47	3.2×10^{-5} (30 °C)
16	PEO/G4/LiTFSI/LLZO	> 0.5	$> 1 \times 10^{-4}$ (20 °C)
17	PVCA-KH570/LLZO	0.752	3.39×10^{-4} (25 °C)

1. H. Y. Huo, X. N. Li, Y. P. Sun, X. T. Lin, K. D. Davis, J. W. Liang, X. J. Gao, R. Y. Li, H. Huang, X. X. Guo, X. L. Sun, *Nano Energy*, 2020, **73**, 104836.
2. Y. Wang, S. Geng, G. Yan, X. Liu, X. Zhang, Y. Feng, J. Shi, X. Qu, *ACS Appl. Energy Mater.*, 2022, **5**, 2495-2504.

3. Y. Wang, H. Ji, X. Zhang, J. Shi, X. Li, X. Jiang, X. Qu, *ACS Appl. Mater. Interfaces*, 2021, **13**, 16469-16477.

4. O. Sheng, C. Jin, J. Luo, H. Yuan, C. Fang, H. Huang, Y. Gan, J. Zhang, Y. Xia, C. Liang, W. Zhang, X. Tao, *J. Mater. Chem. A*, 2017, **5**, 12934-12942.

5. Y. Y. Shi, Z. J. Fan, B. Ding, Z. W. Li, Q. Y. Lin, S. Chen, H. Dou, X. J. Zhang, *J. Electroanal. Chem.,* 2021, **881**, 114916.

6. X. Zhou, X. Li, Z. Li, H. Xie, J. Fu, L. Wei, H. Yang and X. Guo, *J. Mater. Chem. A*, 2021, **9** 18239-18246.

7. J. W. Zha, N. Huang, K. Q. He, Z. M. Dang, C. Y. Shi, R. K. Li, *High Volt.*, 2017, **2**, 25-31.

8. X. Tao, Y. Liu, W. Liu, G. Zhou, J. Zhao, D. Lin, C. Zu, O. Sheng, W. Zhang, H. W. Lee, Y. Cui, *Nano Lett.*, 2017, **17**, 2967-2972.

9. X. Ma, M. Liu, Q. P. Wu, X. Guan, F. Wang, H. M. Liu, J. Xu, *ACS Appl. Mater. Interfaces*, 2022, **14**, 53828-53839.

10. Z. Lu, L. Peng, Y. Rong, E. Wang, R. Shi, H. Yang, Y. Xu, R. Yang, J. Chao, *Energy Environ. Mater.*, 2022, e12498.

11. L. Gao, J. X. Li, J. G. Ju, B. W. Cheng, W. M. Kang, N. P. Deng, *Compos. Sci. Technol.*, 2020, **200**, 108408.

12. R. A. Tong, L. H. Chen, G. Shao, H. L. Wang, C. A. Wang, *J. Power Sources*, 2021, 229672.

13. Q. Zhang, K. Liu, K. Liu, J. P. Li, C. J. Ma, L. Zhou, Y. P. Du, *J. Colloid Interface Sci.*, 2020, **580**, 389-398.

14. L. Chen, Y. T. Li, S. P. Li, L. Z. Fan, C. W. Nan, J. B. Goodenough, *Nano Energy*, 2018, **46**, 176-184.

15. H. Y. Huo, Y. Chen, J. Luo, X. F. Yang, X. X. Guo, X. L. Sun, *Adv. Energy. Mater.*, 2019, **9**, 1804004.

16. M. Falco, L. Castro, J.R. Nair, F. Bella, F. Barde, G. Meligrana, C. Gerbaldi, *ACS. Appl. Energy Mater.*, 2019, **2**, 1600-1607.

17. J. Chai, B. Chen, F. Xian, P. Wang, H. Du, J. Zhang, Z. Liu, H. Zhang, S. Dong, X. Zhou, G.L. Cui, *Small*, 2018, **14**, 1802244.